Poly(vinyl acetate)/Polyacrylate Semi-Interpenetrating Polymer Networks. II. Thermal, Mechanical, and Morphological Characterization

A. Martinelli,[1] L. Tighzert,[2] L. D'Ilario,[1] I. Francolini,[1] A. Piozzi[1]

[1]*Dipartimento di Chimica, Università La Sapienza, Piazzale Aldo Moro 5, 00185 Rome, Italy*
[2]*Ecole Supérieure d'Ingénieurs en Emballage et Conditionnement, Groupe de Recherche en Sciences pour l'Ingénieurs, Laboratoire d'Etudes des Matériaux Polymères d'Emballage, Esplanade Roland Garros, Technopôle Henri Farman, BP 1029, 51686 Reims Cedex, France*

Received 3 March 2008; accepted 4 August 2008
DOI 10.1002/app.29291
Published online 2 December 2008 in Wiley InterScience (www.interscience.wiley.com).

ABSTRACT: The thermal, dynamic mechanical, and mechanical properties and morphology of two series of semi-interpenetrating polymer networks (s-IPNs) based on linear poly(vinyl acetate) (PVAc) and a crosslinked *n*-butyl acrylate/1,6-hexanediol diacrylate copolymer were investigated. The s-IPN composition was varied with different monoacrylate/diacrylate monomer ratios and PVAc concentrations. The crosslinking density deeply affected the thermal behavior. The results showed that a more densely crosslinked acrylate network promoted phase mixing and a more homogeneous structure. The variation in the linear polymer concentration influenced both the morphology and mechanical properties. © 2008 Wiley Periodicals, Inc. J Appl Polym Sci 111: 2675–2683, 2009

Key words: interpenetrating networks (IPN); mechanical properties; morphology; thermal properties

INTRODUCTION

The growing demand for materials for specialty application is frequently not satisfied by one-component systems. As far as polymers are concerned, the development of polymer composites, blends, and copolymers has attracted considerable interest in recent years. Generally, multicomponent polymers, because of a positive free energy of mixing, undergo phase segregation. Thus, to obtain materials with desired properties otherwise not achievable with a single polymer, the phase adhesion, domain size and structure, extent of molecular mixing, and morphology must be controlled.

Particular types of polymer blends in which the phase segregation can be kinetically controlled are interpenetrating polymer networks and semi-interpenetrating polymer networks (s-IPNs).[1] The latter may be obtained by the polymerization of a multifunctional monomer (or by the crosslinking of a functionalized polymer) in the presence of a linear polymer. By the proper selection of the experimental setup, that is, the composition, crosslinking density, polymerization mechanism, kinetics, temperature, and, if used, solvent, different extents of phase mixing can be obtained.

In the first part of this series,[2] we describe the preparation and polymerization kinetics of s-IPNs based on a crosslinked *n*-butyl acrylate (*n*-BA)/1,6-hexanediol diacrylate (HDDA) copolymer network and linear poly(vinyl acetate) (PVAc) and synthesized in bulk by UV photopolymerization. The components of our system were chosen according to the following considerations:

- To obtain transparent films, the refractive indices of the polymers should be very close [refractive index for poly(*n*-butyl acrylate) = 1.466; refractive index for PVAc = 1.467].[3]
- Both polymers have applicatory importance because of their damping properties over a wide temperature range.[4,5]
- The solubility of PVAc in the monomers permits not using a solvent. Moreover, the resulting viscous reaction mixture can be easily spread for coating applications.

In this study, the effects of different concentrations of HDDA (used as a crosslinking agent) and the linear polymer content on the thermal, mechanical, and morphological properties were investigated.

Correspondence to: A. Martinelli (andrea.martinelli@uniroma1.it).

Contract grant sponsor: Ministero dell'Istruzione dell'Università e della Ricerca.

EXPERIMENTAL

s-IPNs, based on a crosslinked *n*-BA/HDDA copolymer and linear PVAc, were synthesized in bulk by UV photopolymerization. Two series of s-IPNs with different crosslinking densities were prepared by the reaction of *n*-BA (Aldrich, St. Louis, MO) and HDDA (Aldrich) in an *n*-BA/HDDA molar ratio of 2 : 1 (s-IPN-A) or 4 : 1 (s-IPN-B) in the presence of different PVAc concentrations (9–28.4 wt %). After the dissolution of PVAc (Aldrich) in the liquid acrylate monomers and complete homogenization of the components, the reaction mixture was poured onto a glass surface and leveled at a fixed height by a roll leaning on two side guides. The curing was carried out in air by irradiation at 305 nm on one sample side with Darocur 1173 (Ciba, Basel, Switzerland) as the photoinitiator. After the films became tack-free, the attenuated total reflection/Fourier transform infrared spectra of the upper and lower film surfaces were acquired with a Golden Gate diamond single reflection device (Specac, Slough, UK). The polymerization reaction was considered concluded when the infrared peak intensity at 810 cm^{-1}, due to the $H_2C{=}CH$ out-of-plane deformation of the acrylate double bonds, of both film surfaces reached a constant value. For all the samples, a reaction conversion of at least 95% was estimated. No remarkable differences were observed between the spectra of the upper and lower film sides. The 75-μm-thick films that were obtained were self-standing, transparent, and macroscopically homogeneous.

The acrylate monomers in the absence of the linear polymer did not polymerize because of the strong inhibition effect of atmospheric oxygen, the diffusion of which inside the reaction mixture was probably hampered by the dissolved PVAc.

The synthesis procedure and polymerization kinetics are described in detail in the first part of this series.[2] Table I summarizes the semi-IPN sample codes and compositions.

For each composition, at least four films were prepared and characterized, and the mean value of the investigated property was reported.

TABLE I
s-IPN Names and Compositions

s-IPN series	Sample	*n*-BA (wt %)	HDDA (wt %)	*n*-BA/HDDA (mol/mol)	PVAc (wt %)
s-IPN-A	A9	45.5	45.5	2	9.0
	A17	41.6	41.6	2	16.8
	A23	38.5	38.5	2	23.0
	A28	35.8	35.8	2	28.4
s-IPN-B	B9	63.7	27.3	4	9.0
	B17	58.4	24.8	4	16.8
	B23	53.8	23.2	4	23.0
	B28	50.2	21.4	4	28.4

Characterization

Thermal analysis

Differential scanning calorimetry (DSC) analysis was carried under N_2 with a Mettler TA-3000 DSC apparatus (Mettler-Toledo, Schwerzenbach, Switzerland) from −150 to 150°C. The scan rate used for the experiments was 20 K/min, and the sample weight was about 8–9 mg. The glass-transition temperature (T_g) values of the samples were taken as the transition inflection point determined in the first derivative plot of the DSC curve.

Mechanical testing

To evaluate the sample tensile properties, the standard test method ASTM D 882-97 was used. Stress–strain curves were recorded with an Instron 4502 (Bucks, UK) test machine with a crosshead speed of 5 mm/min on 10 × 50 × 0.075 mm^3 films. The strain values were reported as ΔL (elongation)/L_0 (sample length).

Dynamic mechanical thermal analysis (DMTA)

DMTA was carried out in the tensile mode with a Rheometrics RSA II solid analyzer (Piscataway, NJ). The real component [storage modulus (E')] and imaginary component [loss modulus (E'')] of the complex tensile modulus and the loss factor ($\tan\delta = E''/E'$) were investigated through the heating of the sample at 5 K/min from −80 to 80°C at a test frequency of 1 Hz with 0.05% dynamic deformation.

Morphology

For the morphological observations, which were carried out with a Leo 1450VP Inca 300 scanning electron microscope (Thornwood, NY), the samples were fractured in liquid nitrogen and coated with gold. The scanning electron microscopy (SEM) analysis was also carried out on samples that were extracted with tetrahydrofuran (THF) to etch out the PVAc-rich phase.

RESULTS AND DISCUSSION

In the first part of this series,[2] which deals with s-IPN synthesis, it is shown that the PVAc and crosslinking agent (HDDA) concentrations greatly influence the acrylate polymerization kinetics. In particular, increasing either the amount of PVAc or HDDA in the reaction mixture increases the network formation rate. s-IPN-A reacts systemically faster than s-IPN-B.

The different s-IPN compositions (i.e., the different crosslinking densities and PVAc concentrations) and the different kinetics modify the sample phase segregation and hence the thermal, morphological, and mechanical properties.

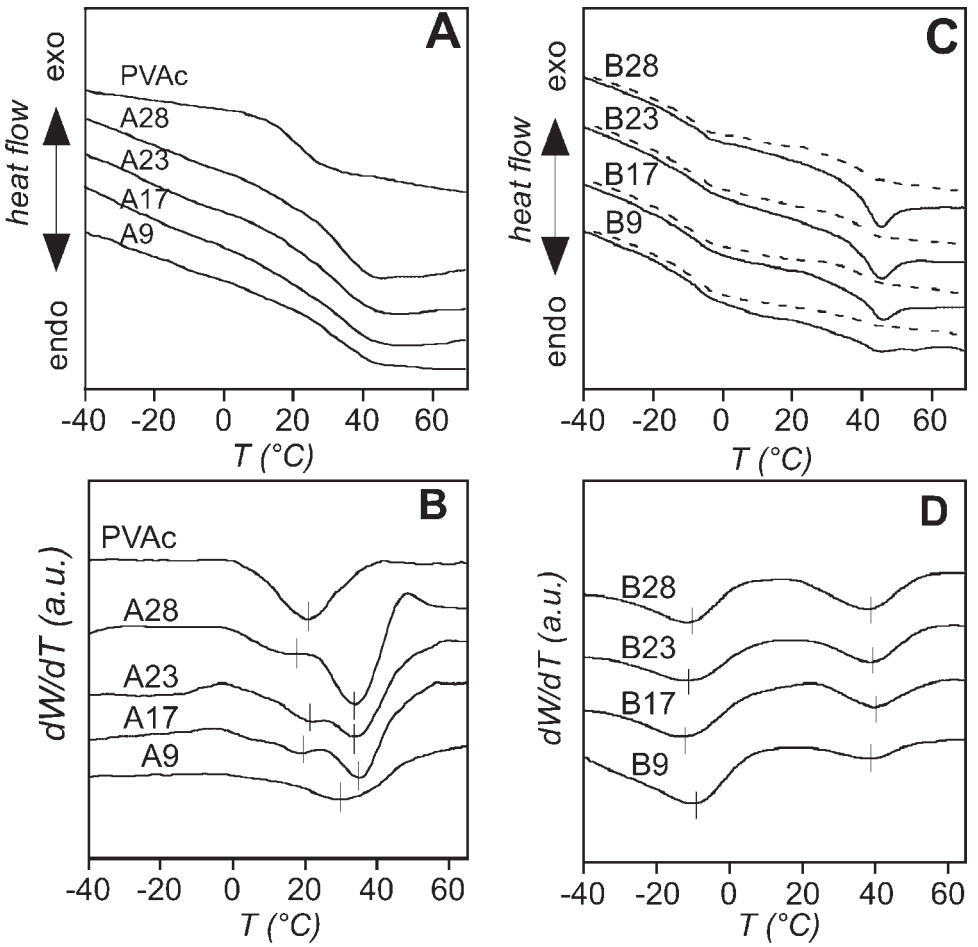

Figure 1 DSC thermograms of the linear polymer and s-IPNs [(A) PVAc and s-IPN-A and (C) s-IPN-B for (—) the first and (- - -) second heating runs] and first derivatives of DSC curves [(B) PVAC and s-IPN-A and (D) s-IPN-B for the second heating run]. T is the temperature and W is the heat flow in Watt.

After photopolymerization and vacuum drying, transparent and macroscopically homogeneous 75-μm-thick s-IPN films were characterized with DSC, DMTA, SEM, and mechanical tests, the results of which are discussed hereafter.

DSC

In Figure 1 (A), the DSC thermograms of PVAc and s-IPN-A samples are reported. The linear polymer shows a glass transition between about 10 and 30°C, which is centered at the PVAc T_g value of 21°C.

For the s-IPN-A samples, the thermograms reveal a broad transition spanning over a wide temperature range (10–45°C). With the exclusion of sample A9, the total specific heat increase (ΔC_p) is composed of two overlapping jumps centered at about 20 (defined as the lower T_g value) and 34°C (defined as the upper T_g value). This is shown more clearly in Figure 1(B), in which the first derivatives of the DSC curves are reported to examine the existence of the two glass transitions. They are strictly related to the linear polymer. In fact, upon sample extraction with THF, which is a PVAc solvent, ΔC_p at T_g drastically decreases, appearing in the thermogram as a flat inflection at about 25°C. As an example, the DSC profile variation of sample A28 before and after THF extraction is reported in Figure 2.

The absence of any other transition up to 150°C, the temperature at which PVAc degrades, reveals that in the densely crosslinked acrylate network, the chain segments between the junction points are not long enough to relax. We can assign the lower temperature transition of the s-IPN-A samples [Fig. 1(A,B)] to T_g of free PVAc domains segregated from the acrylic polymer. The upper temperature transition of the A series s-IPNs [Fig. 1(A,B)] may be associated with a mixed phase in which the cooperative long-range segmental motion of linear polymer chains, confined within the acrylic rigid network, is restricted. A similar antiplasticization effect of poly(butyl acrylate) (PBA) was also observed by Pathmanathan et al.[6] in a 50/50 PVAc/PBA blend and was related to partial homogeneous mixing of the two polymers.

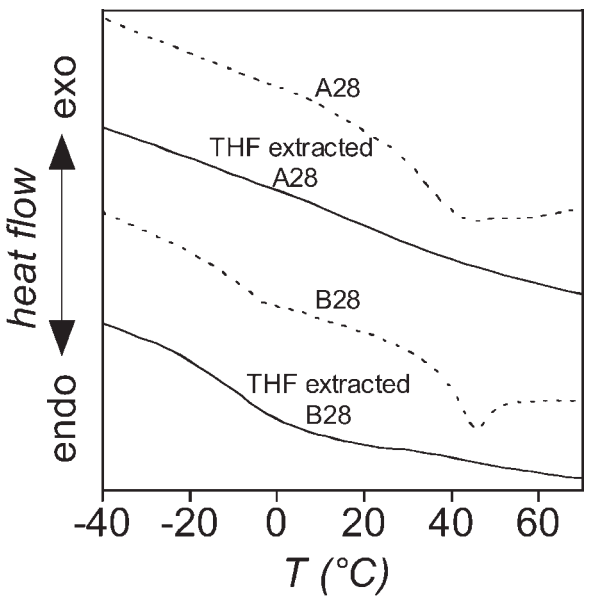

Figure 2 DSC thermograms of (- - -) pristine and (—) THF-extracted A28 and B28. T is the temperature.

Two well-separated transitions can be observed in the DSC thermograms of s-IPN-B, which is characterized by a lower crosslink density [Fig. 1(C,D)]. Although T_g is unknown because of the impossibility of obtaining such a polymer in air (our experimental condition), the lower temperature transition shown in Figure 1(C) (≈−10°C) can be attributed to an acrylate-rich phase. In fact, a steady increase in T_g of PBA upon crosslinking has been reported in the literature:[7] when the polymer was crosslinked with 4 mol % tetraethylene glycol dimethacrylate, its T_g increased from −55[8] to −13°C, as measured in dynamic mechanical experiments.

Moreover, after the dissolution of the linear polymer by Soxhlet THF extraction of sample B28, the resulting very brittle, disaggregated material shows only the lower T_g (Fig. 2).

The higher T_g value is superimposed to an endothermic peak due to an enthalpy relaxation process taking place at room temperature after the sample synthesis. To better assign the transition temperature, a second heating scan was carried out to erase the sample thermal history [the dotted line in Fig. 1(C)]. The higher T_g was attributed to a mixed phase rich in the linear polymer, which, like that in s-IPN-A, is stiffened by the acrylate network and disappears upon THF extraction (Fig. 2). This relaxation, independent of the semi-IPN composition, is characterized by an inflection point at about 40°C and an end point at 45°C [Fig. 1(C,D)]. Moreover, the segregated linear polymer relaxation, except for a very small inflection at 21°C in sample B28, was no longer observable [Fig. 1(C)].

DMTA

The dynamic mechanical properties of s-IPN-A and s-IPN-B are shown in Figure 3, in which the temperature dependence of E' and tan δ is reported. For the sake of comparison, the tan δ intensity of PVAc has been reduced by a factor of 2. In agreement with the glass transition of the linear polymer, the s-IPN-A samples also show an α relaxation [at the α-

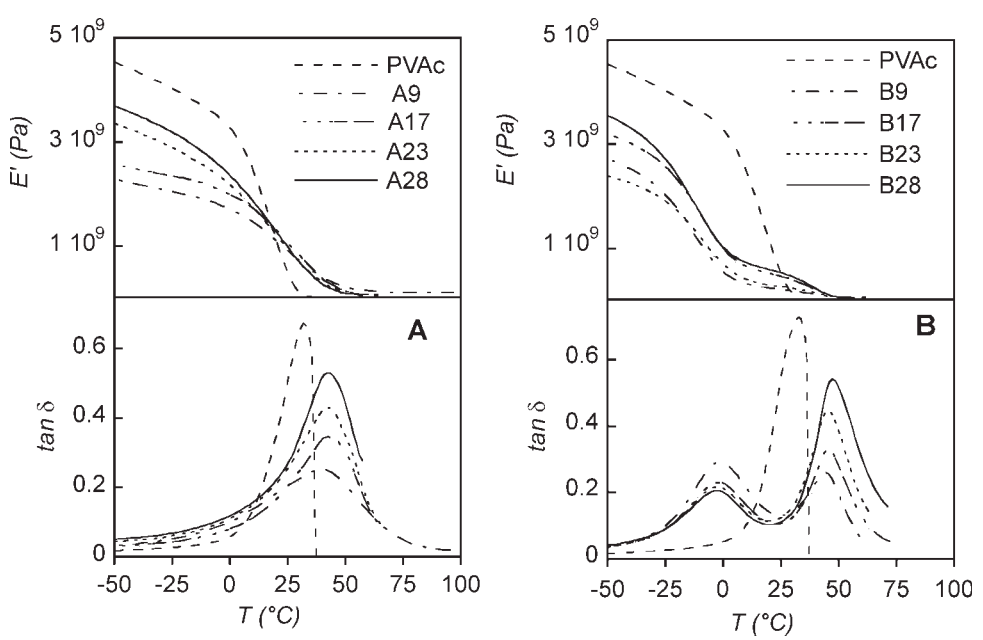

Figure 3 Temperature (T) dependence of E' and tan δ of (A) PVAc and s-IPN-A and (B) s-IPN-B samples with different PVAc contents.

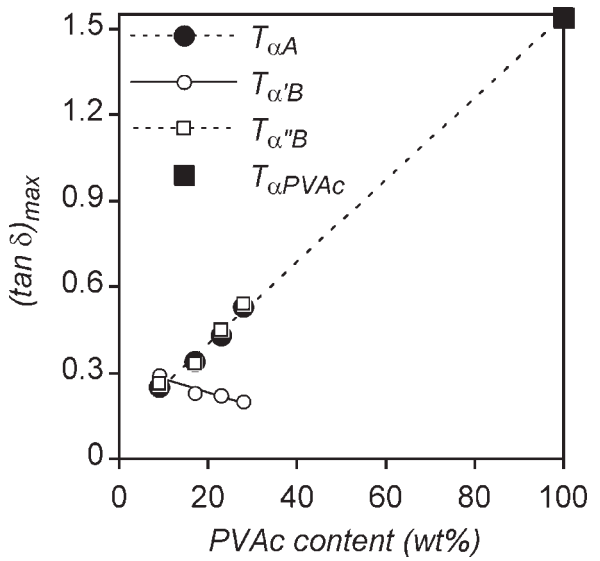

Figure 4 Tan δ peak height variation as a function of the PVAc concentration in PVAc, s-IPN-A, and s-IPN-B.

relaxation temperature of s-IPN-A ($T_{\alpha A}$)] characterized by a drastic E' drop and a tan δ peak.

At a low temperature, before the α-relaxation temperature (T_α), the linear polymer behaves more rigidly than the s-IPNs, showing the highest E' value. In s-IPNs, it decreases as the acrylic polymer concentration increases. The opposite trend can be observed at a temperature above the glass transition. In fact, because of the large amount of creeping after the α relaxation, the tan δ peak of PVAc was not completely recorded. The presence of the acrylic three-dimensional network suppresses the drastic modulus drop at T_α, and the dynamic mechanical behavior of the s-IPNs may be followed at a higher temperature. The E' value of sample A28 in the rubbery state at 70°C is 1×10^8 Pa, twice that of those of the other s-IPN-A samples. The maximum of the tan δ peak is at about 33°C for PVAc and at about $T_{\alpha A} = 41$–43°C for s-IPN-A and does not vary with changes in the composition. As shown in Figure 4, the tan δ peak height linearly increases with the PVAc concentration.

As expected from DSC experiments, the dynamic mechanical analysis of s-IPN-B samples shows two well-defined relaxations, α'_B and α''_B. The tan δ peaks, centered at about −3 [α'_B-relaxation temperature ($T_{\alpha' B}$)] and 47°C [α''_B-relaxation temperature ($T_{\alpha'' B}$)], as reported in the DSC result analysis regarding such transitions, have been assigned to the glass transition of the acrylate network and the acrylate/PVAc mixed phase, respectively. The tan δ peak intensities of α'_B and α''_B are linearly related to the acrylate and PVAc content in the s-IPNs, respectively (Fig. 4).

To compare the dynamic mechanical behavior of the two s-IPNs, the tan δ values versus the temperature for samples A23 and B23 are reported in Figure 5.

The less densely crosslinked sample (B23) shows a symmetric damping α''_B peak with a half-height width (full width at half-maximum) of 14°C. The shape of the A23 tan δ peak is large (full width at half-maximum = 22°C) and asymmetric, with a broad hump on the low temperature side. This may due to the local structural heterogeneity and to the relaxation of a PVAc fraction partially segregated from the network, which was also found in the DSC analysis.

SEM

The morphology of the s-IPNs was investigated with SEM. Figures 6 and 7 show fracture-surface micrographs of s-IPN-A and s-IPN-B samples as prepared and extracted with THF for the removal of the PVAc-rich phase.

Nonextracted and extracted A9 and B9 samples [Fig. 6(A,B) and 7(A,B)] show a vague structure without any marked evidence of phase separation. No drastic changes can be observed for the extracted samples.

As the linear polymer content in the s-IPN-A samples increases, the morphology progressively assumes a granular structure, which is well defined in A28 [Fig. 6(G)], and it does not undergo marked modifications after the THF extraction. This observation, together with the thermal analysis results, strengthens the more homogeneous structure model for s-IPN-A.

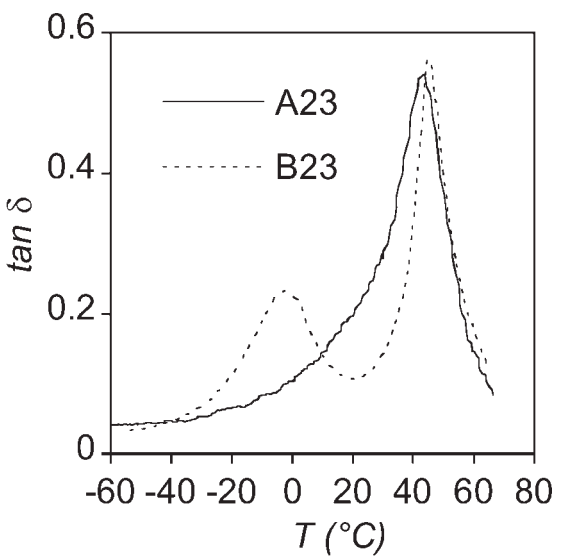

Figure 5 Comparison of the dynamic mechanical behavior of s-IPNs with different crosslinking densities: tan δ versus the temperature (T) for (—) A23 and (- - -) B23 samples.

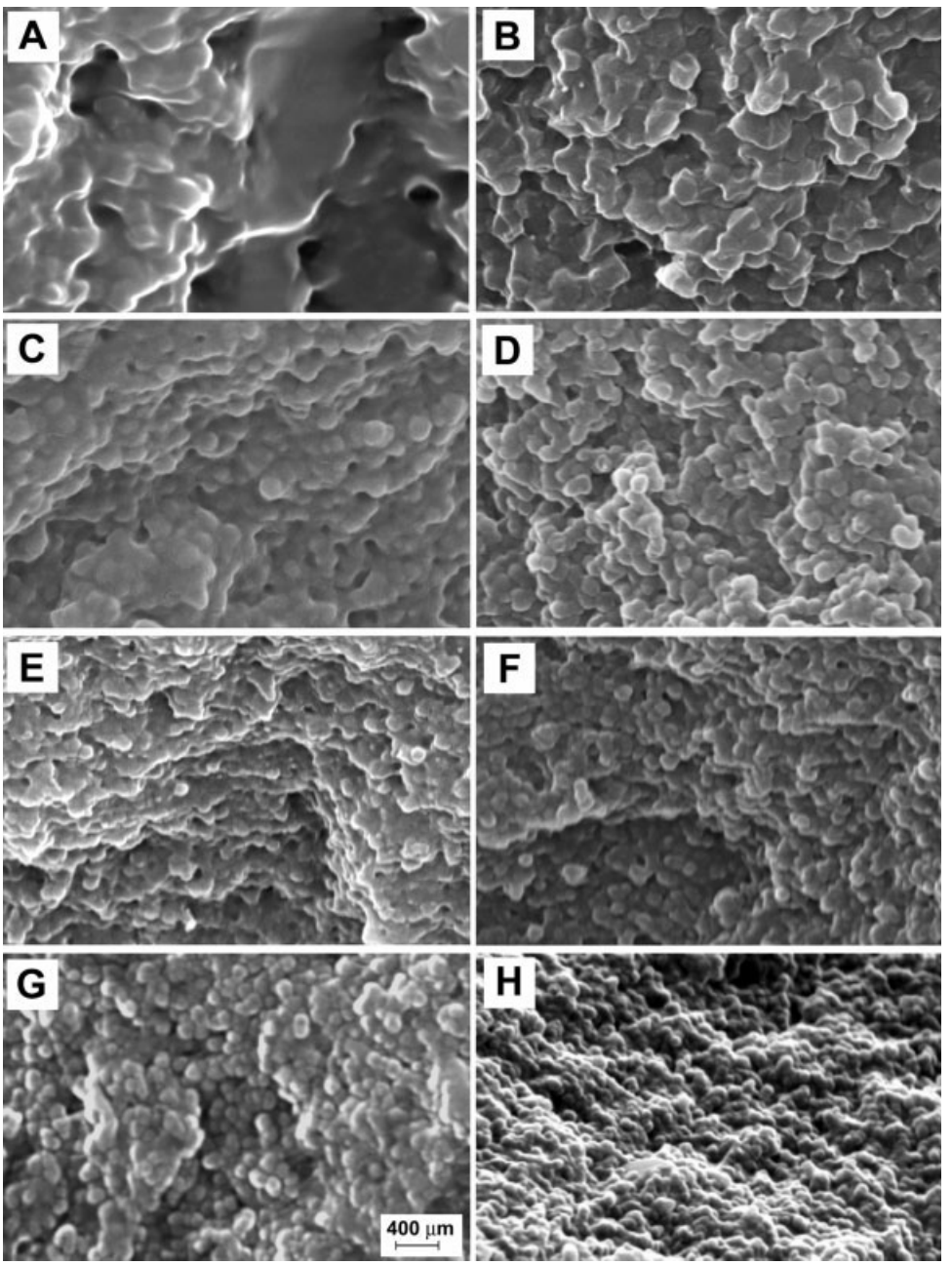

Figure 6 Fracture-surface SEM micrographs of s-IPN-A samples: as prepared [(A) A9, (C) A17, (E) A 23, and (G) A28] and extracted [(B) A9, (D) A17, (F) A 23, and (H) A28]. The bar represents 400 μm.

With the linear polymer concentration increasing, the average size of the connected globular domains decreases from 230 nm for sample A17 to 130 nm for sample A28.

The granular structure of the s-IPN-A samples in less densely crosslinked s-IPN-B is completely wrapped in a continuous phase; this is very clear in the samples with the higher PVAc content [B23 and B28; Fig. 7(E,G)]. Spheroidal particles can be clearly highlighted after the THF extraction [Fig. 7(F,H)].

In the densely crosslinked semi-interpenetrating network (s-IPN-A), both the small acrylate network mesh and the fast reaction hinder polymer segregation, which presumably takes place only in the last polymerization stage. On the other hand, in s-IPN-B, as the polymerization and crosslinking reaction start, the incompatible PVAc has sufficient mobility and time to segregate during the acrylate network formation. Such a process gives rise to a material composed of insoluble, crosslinked acrylate-rich beads surrounded by a continuous PVAc-rich phase.

Before and after THF extraction, the weight loss of all s-IPN samples was evaluated, and the results are reported in Figure 8 as a function of the PVAc content. The dotted line represents the expected amount of solubilized PVAc (slope = 1).

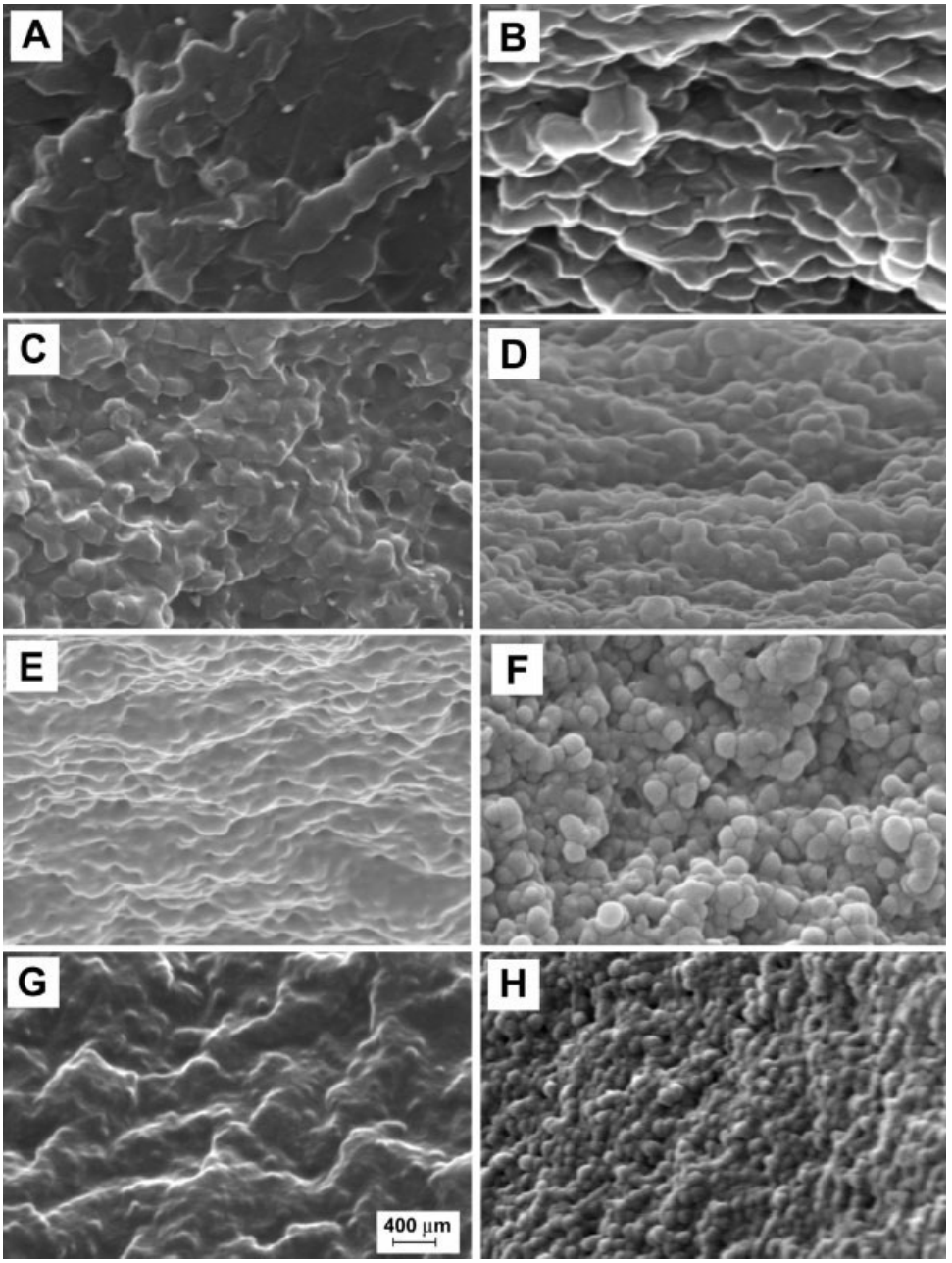

Figure 7 Fracture-surface SEM micrographs of s-IPN-B samples: as prepared [(A) B9, (C) B17, (E) B23, and (G) B28] and extracted [(B) B9, (D) B17, (F) B23, and (H) B28]. The bar represents 400 μm.

In agreement with the previous results, it can be observed that in s-IPN-A the extraction cannot completely solubilize the linear polymer, which partially remains in the tight acrylate meshes. On the contrary, in s-IPN-B, the dissolved amount is higher than expected, probably because of partial solubilization of a less crosslinked acrylate fraction.

Mechanical properties

The tensile behavior of PVAc and s-IPNs was investigated at a strain rate of 5 mm/min at room temperature. Some stress–strain curves up to a strain of 0.05 and the variation of Young's modulus (determined as the maximum slope of the curve) as a function of the PVAc content are displayed in Figures 9 and 10(A), respectively. In the inset of Figure 9, the mechanical behavior of PVAc is reported.

The s-IPNs do not exhibit any evident yield point or necking during the tensile experiments. To characterize the viscous behavior of the s-IPNs, the offset yield strength at an elongation of 0.02 was followed, and the data are displayed in Figure 10(B).

As far as the stress and strain at the break are concerned, great data dispersion and no direct relation with the PVAc concentration for the same s-IPN

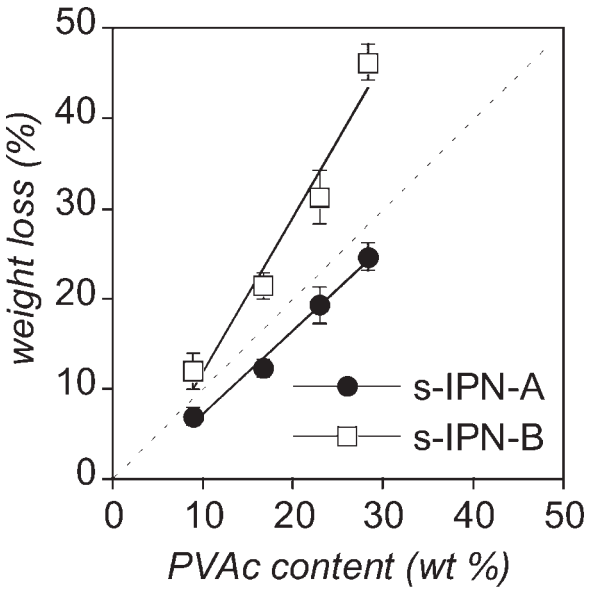

Figure 8 Sample weight loss upon THF extraction as a function of the PVAc content.

series have been found. In general, the s-IPN-A samples show a greater ultimate strength and lower elongation at break than s-IPN-B.

PVAc shows at room temperature, close to its T_g, a low Young's modulus of 22 MPa and tensile strength of 0.3 MPa, a high elongation at break of 200%, and a very broad not well-defined yield point. Despite its scarce mechanical properties, PVAc produces a synergistic reinforcing effect when mixed with the acrylic network in the s-IPNs. In fact, as shown in Figure 10, with the linear polymer concentration increasing, the Young's modulus and the offset strength increase in both semi-interpenetrating networks.

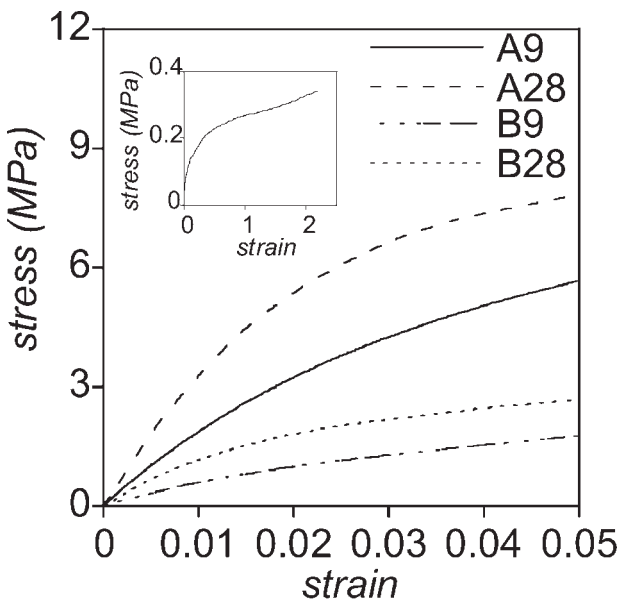

Figure 9 Some stress–strain curves up to a strain of 0.05 for some selected samples. In the inset, the mechanical behavior of PVAc is presented.

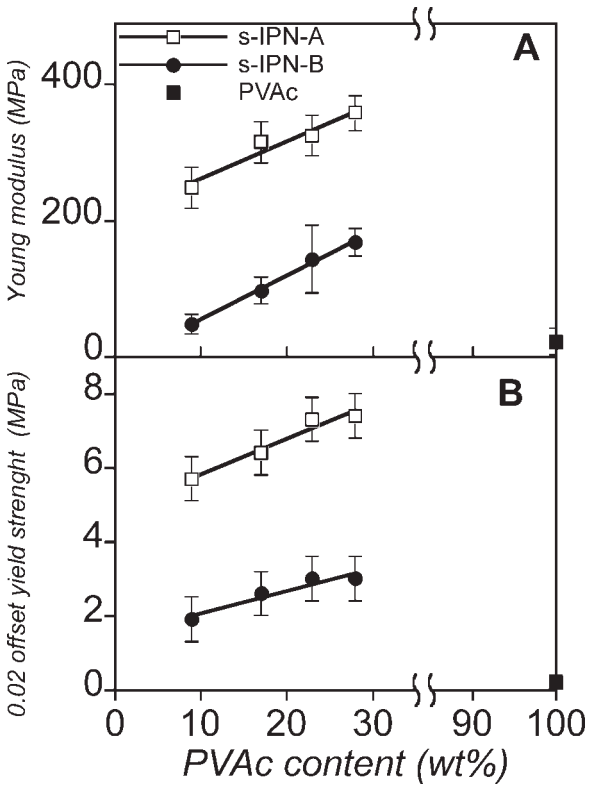

Figure 10 Mechanical properties of PVAc, s-IPN-A, and s-IPN-B samples: (A) Young's tensile modulus and (B) offset yield strength at an elongation of 0.02 as a function of the PVAc content.

This synergistic effect has also been observed in other immiscible blends and in general has been attributed to different causes, such as strong polymer interpenetration in the phase interface,[9] blending-induced changes in the specific volume,[10] and the formation of a strong interaction between the component polymers.[11] In addition, the behavior observed in our samples (Fig. 10) can be explained by the fact that the PVAc-rich phase in s-IPNs is in the glassy state and thus contributes to the increase in the sample stiffness, its T_g being above room temperature. Moreover, a systematically higher rigidity can be recorded for s-IPN-A (Fig. 10). The different morphologies of the s-IPNs, as revealed by electron microscopy, can explain this experimental evidence. In fact, s-IPN-A shows more marked phase continuity, a result of a more homogeneous structure. In the s-IPN-B samples, the discontinuous, rigid acrylate-rich phase segregates from more compliant, continuous PVAc-rich domains, which more easily yield when stressed.

CONCLUSIONS

DSC, DMTA, SEM, and mechanical tests were employed to study the effect of the PVAc

concentration on the behavior of two s-IPN series that were characterized by different monoacrylate/diacrylate monomer ratios.

It was observed that the crosslink density plays the main role in defining the material properties; meanwhile, inside each s-IPN series, the properties change smoothly with the linear polymer concentration.

According to the experimental results, it has been proposed that more densely crosslinked s-IPN-A exhibits greater phase mixing, the small acrylate network mesh partially hampering the linear polymer segregation. On the contrary, in less densely crosslinked s-IPN-B, PVAc has sufficient mobility to segregate during the formation of the acrylate network and can be completely solubilized in THF. These different s-IPN structures directly influence the mechanical behavior of the material. Tensile stress–strain tests showed that the s-IPN-A samples were systematically more rigid than the s-IPN-B ones.

The authors thank Silvia Vicentini for her useful experimental work.

References

1. Sperling, L. H.; Mishra, V. Polym Adv Technol 1996, 7, 197.
2. Martinelli, A.; Tighzert, L.; D'Ilario, L.; Francolini, I.; Piozzi, A. J Appl Polym Sci 2008, 111, 2669.
3. Seferis, J. C. In Polymer Handbook, 3rd ed.; Brandrup, J.; Immergut, E. H., Eds.; Wiley: New York, 1989.
4. Chu, H.-H.; Lee, C.-H.; Huang, W. G. J Appl Polym Sci 2004, 91, 1396.
5. Mathew, A.; Deb, P. C. J Appl Polym Sci 1992, 45, 2145.
6. Pathmanathan, K.; Cavaille, J. Y.; Johari, G. P. Polymer 1988, 29, 311.
7. Chan, M. C. O.; Thomas, D. A.; Sperling, L. H. J Appl Polym Sci 1987, 34, 409.
8. Gaur, U.; Lau, S.-F.; Wunderlich, B. B.; Wunderlich, B. J Phys Chem Ref Data 1982, 11, 1065.
9. Chang, F.-C.; Yang, M.-Y.; Wu, J.-S. Polymer 1991, 32, 8.
10. Ramiro, J.; Eguiazabal, J. I.; Nazabal, J. Polym Adv Technol 2003, 14, 129.
11. Sivalingam, G.; Karthik, R.; Madras, G. Polym Degrad Stab 2004, 84, 345.